IEEE Photonics Journal
An IEEE Photonics Society Publication

Exploring Waveguiding Properties of Heavily Doped $Yb^{3+}:KLu(WO_4)_2$ Epitaxial Layers

Volume 2, Number 3, June 2010

Western Bolaños, Member, IEEE
Joan J. Carvajal
Xavier Mateos
Magdalena Aguiló
Francesc Díaz

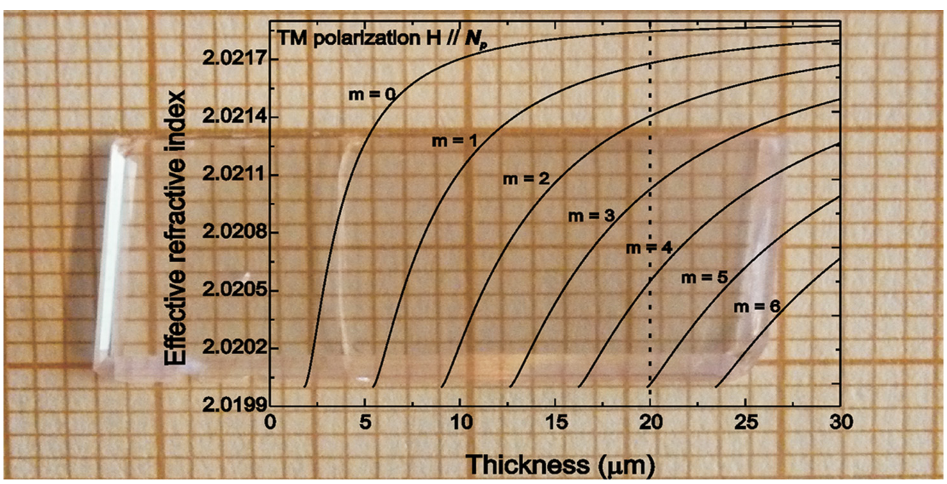

DOI: 10.1109/JPHOT.2010.2050580
1943-0655/$26.00 ©2010 IEEE

Exploring Waveguiding Properties of Heavily Doped Yb^{3+}:$KLu(WO_4)_2$ Epitaxial Layers

Western Bolaños, *Member, IEEE*, Joan J. Carvajal, Xavier Mateos, Magdalena Aguiló, and Francesc Díaz

Física i Cristal lografía de Materials i Nanomaterials (FiCMA-FiCNA), Universitat Rovira i Virgili (URV), 43007 Tarragona, Spain

DOI: 10.1109/JPHOT.2010.2050580
1943-0655/$26.00 ©2010 IEEE

Manuscript received April 9, 2010; revised May 10, 2010; accepted May 10, 2010. Date of publication May 12, 2010; date of current version June 11, 2010. This work was supported by the Spanish Government under Project MAT 2008-06729-C02-02/NAN and Project PI09/90527 and the Catalan Government under Project 2009SGR235. The work of W. Bolaños was supported by the Catalan Government with funds provided through the fellowship 2009FI-B 00430. J. J. Carvajal was supported by the Education and Science Ministry of Spain and European Social Fund under the Ramon y Cajal program, RYC2006-858. Corresponding author: J. J. Carvajal (e-mail: joanjosep.carvajal@urv.cat).

Abstract: High-quality epitaxial layers of heavily doped Yb:$KLu(WO_4)_2$ grown on $KLu(WO_4)_2$ substrates by liquid phase epitaxy were characterized in terms of lattice mismatch and refractive indexes of the layer and the substrate. The effective refractive indexes of the guided modes that these structures can support were modeled and measured experimentally for the transverse electric (TE) and transverse magnetic (TM) mode excitation by dark m-lines spectroscopy. The upper limit for optical losses in these waveguides corresponding only to scattering processes was estimated to be $\sim$1.5 dB/cm at $\lambda = 632.8$ nm. These results show that, apart for highly efficient thin-disk laser applications, these epilayers can be used as waveguide devices at wavelengths different from those used to excite Yb^{3+}.

Index Terms: Epitaxial growth, dielectric films, optical planar waveguides.

1. Introduction

The study of optical, structural and thermomechanical properties of monoclinic $KLu(WO_4)_2$ single crystals had demonstrated its effectiveness as gain media for active lanthanide ions [1]–[4]. Indeed, the spectroscopy and laser operation of Yb^{3+} [5], [6], Tm^{3+} [7], Er^{3+} [8], Ho^{3+} [9], and Nd^{3+} [9], [10] in the KLuW host (the abbreviation of $KLu(WO_4)_2$ adopted hereafter) have already been reported. However, Yb^{3+} doped crystals have emerged as an interesting alternative to Nd^{3+} laser systems for high power applications, as well as for their capability to generate ultra short laser pulses. In spite of the fact that other crystals of the family of rare earth monoclinic double tungstates, such as $KY(WO_4)_2$ and $KGd(WO_4)_2$, have also been doped with Yb^{3+} [11], KLuW crystals are more suitable to be doped with Yb^{3+} since the smallest difference of ionic radii between Yb^{3+} and each of the Lu^{3+}, Y^{3+}, and Gd^{3+} ions is precisely that one which corresponds to the pair $Lu^{3+}-Yb^{3+}$ (only 0.008 Å compared with 0.034 Å between $Y^{3+}-Yb^{3+}$ and 0.068 Å between $Gd^{3+}-Yb^{3+}$). This, together with the relative large ion separation of lanthanide elements in the monoclinic double tungstate hosts allows working with high doping levels of Yb^{3+} (up to 75%) while still maintaining a good optical and structural quality of the crystal, and without observing quenching of luminescence due to concentration.

In addition to this, high doping levels of Yb^{3+} in the KLuW host, the high absorption and emission cross sections, the short absorption length, and the extremely small laser quantum defect have allowed the demonstration of very efficient laser generation in both bulk [4]–[6] and thin-films [12], [13], including the thin-disk laser configuration [14].

This family of materials have already attracted attention for integrated optical applications, and Romanyuk *et al.* [15] demonstrated the laser operation of an Yb^{3+} based planar waveguide in monoclinic double tungstates for the first time in 2006. They grew a high-quality 1.2 at.% Yb^{3+}:KYW epitaxial layer on a KYW substrate, achieving continuous wave laser operation near 1 μm with an output power of 290 mV and a slope efficiency of around 80% when pumped at 980.5 nm. More recently, Bain *et al.* [16] have also reported a Yb^{3+}: KYW planar waveguide laser, and in addition to the continuous wave regime, they reported the Q-switched operation of a 3 at.% Yb^{3+}: KYW epitaxial layer grown on KYW substrate by using a semiconductor saturable absorber mirror.

Apart from demonstrating guiding laser operation in these materials, it would be interesting to explore the possibilities they offer to guide the light generated by other elements of an integrated optics circuit. This means to explore their possibilities to act as passive waveguides with reduced losses that can act as interconnects between different active elements of a possible integrated optics circuit based on this family of materials. For that, a material with a reduced number of optical transitions that involve absorption and emission processes along its transparency window is required. In this way, the range of wavelengths that can be used for passive waveguiding can be maximized. According to this criterion, among the different members of the monoclinic double tungstates family that form a solid solution of isostructural materials, KLuW, KYW, and KGdW would be preferred since they do not present optical transitions in the entire transparency window of these materials. However, it is also necessary to have a combination of epitaxial layer/substrate that shows a small lattice mismatch so that the epilayer can be grown with high quality on that substrate, and then, scattering optical losses due to crystallographic defects generated at the interface between the epitaxial layer and the substrate can be reduced. This point is impossible to achieve only with combinations of the three members of this family mentioned above. Apart from these ions, the other lanthanide ion that is showing a reduced number of optical transitions in the transparency window of this family of materials is Yb^{3+} due to its simple energy level scheme formed only by the fundamental $^2F_{7/2}$ and the excited $^2F_{5/2}$ states. Then, the election of the epitaxial layer/substrate pair is clear: Yb^{3+}: KLuW/KLuW will be the combination that will show the smallest lattice mismatch among the rest of the members of the monoclinic double tungstates family [17]. Apart from that, the analysis of the refractive index of different members of this family of materials shows that it would be possible to get a refractive index contrast with this epilayer/substrate pair high enough to allow light to be confined in the epitaxial layer, since the introduction of Yb^{3+} in these crystals increases their refractive indexes [18]. So, an unexplored but interesting application of highly doped Yb^{3+}: KLuW thin films would be passive waveguiding at wavelengths that do not imply excitation of Yb^{3+} ions, i.e., the regions between 350–900 nm and 1030–4500 nm, which include the three IR windows of optical communications [19].

We have shown previously that high-quality epitaxial layers of Yb^{3+}: KLuW can be grown on KLuW substrates [12]–[14]. In this work, we show how the heavily doped Yb:KLuW epilayers grown on KLuW substrates by liquid phase epitaxy (LPE) can also be used as efficient passive planar waveguides for wavelengths that do not imply the excitation of Yb^{3+}.

2. Epitaxial Growth and Characterization of the Epitaxial Films

The substrates over which 50 at.% Yb:KLuW epitaxial layers have been grown were obtained from bulk undoped KLuW single crystals. These bulk single crystals were grown in a vertical tubular furnace by the high temperature Top Seeded Solution Growth (TSSG) technique, with a slow cooling of the solution. The solution of growth for bulk single crystals was prepared in Pt crucibles by mixing 88 mol% of $K_2W_2O_7$, used as solvent, and 12 mol% of solute (KLuW). The KLuW single crystals were grown on crystallographic **b**-oriented crystal seeds. Further details on the growth conditions of these crystals can be found in [4]. The as grown crystals were colorless, transparent, and free of macroscopic defects and inclusions and had dimensions of about $23 \times 9 \times 12$ mm^3 along the $\mathbf{c} \times \mathbf{a}^* \times \mathbf{b}$ crystallographic directions and weights of about 14 g. We cut them into

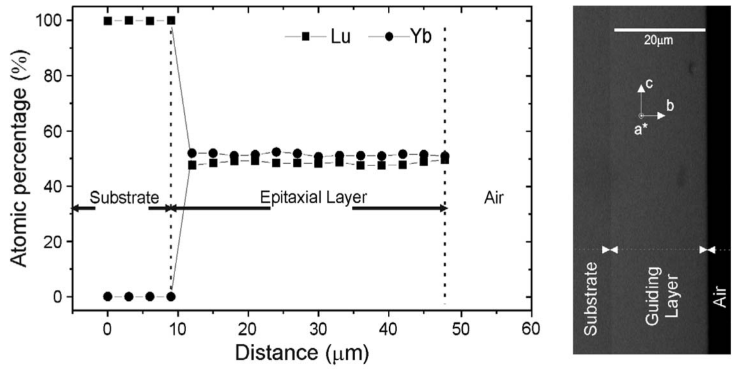

(a) (b)

Fig. 1. Scheme of the atomic percentage of Lu and Yb across the substrate and epitaxial layer calculated from the EPMA results. The ESEM picture shows the substrate/epitaxial layer interface, taken using backscattered electrons.

2.0-mm-thick plates perpendicular to the **b** crystallographic direction and polished to top and bottom faces of each plate with alumina powders to a grain size of 0.3 μm.

The 50 at.% Yb:KLuW layers were grown on these substrates by LPE. The solution of growth was prepared at the molar ratio solute/solvent 7/93 using $K_2W_2O_7$ as solvent. With this solution composition, we had a better control on the supersaturation of the solution, as described by the solubility curves in [17] and, consequently, on the growth rate and thickness of the epilayer obtained. We proceeded with the growth process at a supersaturation level of 5.3% over 2 h. A detailed description of the growth process of these epitaxial layers can be found in [13]. We obtained high-quality and crack-free epitaxial layers, with a typical thickness of 50 μm after growth. By means of electron probe microanalysis we determined the chemical composition of the substrate as well as the epitaxial layers, as can be seen in Fig. 1.

The distribution coefficient for both Lu^{3+} and Yb^{3+} was close to the unity in the substrate and in the epitaxial layer. The sharp change in the concentration of the Yb^{3+} at the interface between the epilayer and the substrate indicated that there was no diffusion of Yb^{3+} ions into the substrate. This observation was confirmed by the ESEM picture in Fig. 1(b). The concentration of Yb^{3+} did almost not change along the epitaxial layer, which indicated that the doping level of the epitaxial layer was uniform. The composition of the epitaxial layer we determined from EPMA results was $KLu_{0.49}Yb_{0.51}(WO_4)_2$, which means that the concentration of Yb^{3+} in these epilayers was 3.35×10^{21} ions/cm^3.

The crystalline quality of the epitaxial layer was investigated by means of X-ray diffraction (XRD) measurements. Monoclinic double tungstates crystallize with the spatial group of symmetry C2/c. A Bruker-AXS D8-Discover with parallel incident beam (Göbel mirror) and vertical goniometer was used for this purpose, equipped with a collimator for the X-ray beam of 500 μm and a GADDS detector. The GADDS detector was 30×30 cm^2 with a 1024×1024 pixel CCD sensor. Cu radiation was obtained from a copper X-ray tube operated at 40 kV and 5 mA. First, a 2θ scan was recorded on the epilayer in order to check the orientation of the thin film. Data were recorded in two different steps with the area detector by performing an ω-scan with a frame width of 15° in the θ range 5°–35° with an integration time of 60 s/frame. After that, an XRD ω-scan (rocking curve) was recorded on the surfaces perpendicular to the **b** direction, both for the substrate and the epilayer, in order to determine its crystalline quality of the film grown. This was done in this way because the film was too thick to record simultaneously the rocking curve for the substrate and the epitaxial layer. Data were recorded for the (040) reflection at $2\theta = 17.82°$, in the ω range 16.32°–19.32°, in 150 frames, with a frame width of 0.02° and an integration time of 5 s/frame. The results of XRD characterization are shown in Fig. 2.

From the 2θ scan in Fig. 2 (see inset) we were able to identify the (020), (040), and (060) reflections of the structure of KLuW substrate and 50 at.% Yb:KLuW epitaxial film, which correspond to the $(0k0)$ reflections, indicating that effectively, the epitaxial film was oriented parallel to the plane (010) or/and perpendicular to the **b** direction, as expected.

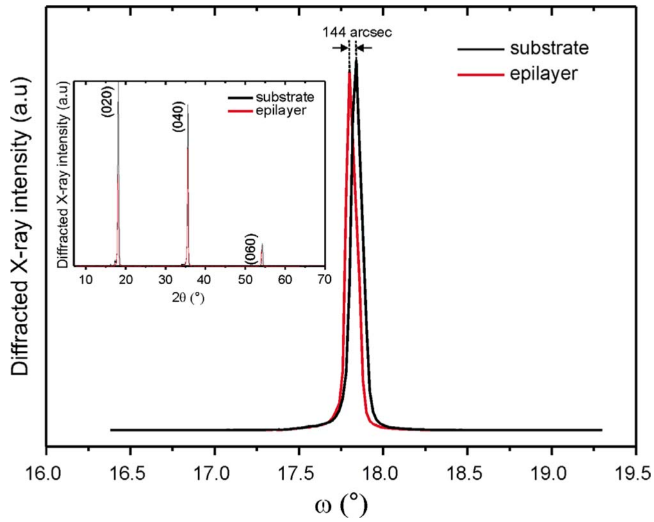

Fig. 2. Rocking curve corresponding to (040) peak determined by X-ray diffraction pattern of Yb:KLuW grown on KLuW substrate, which is shown in the inset.

As can be seen from the rocking curve in Fig. 2, the peaks recorded for the substrate and the epilayer corresponding to the (040) reflection are sharp and narrow, indicating that the film has high crystalline quality comparable to that of the substrate. The FWHM of the layer peak was found to be 260 arcsec, which is close to that one of the substrate peak, i.e., 277 arcsec. The perpendicular lattice mismatch of the film with respect to the substrate, $(\Delta b/b)$, was calculated from the separation $(\Delta\theta)$ between the substrate and the layer peaks, using the Bragg law in differential form $(\Delta b/b) = -(\Delta\theta)\cdot(\cot\theta_B)$, where θ_B is the Bragg angle for the reflection used [20]. In our epitaxy, we determined a lattice mismatch of -2.17×10^{-3}, which is in well agreement with that one calculated from the lattice parameters of KLuW and 50 at.% Yb:KLuW crystals [4] obtained by X-ray powder diffraction measurements $(\Delta b/b) = (b_{KLuW} - b_{Yb:KLuW})/(b_{KLuW}) = -1.80\times10^{-3}$. The small difference between these two values is due to the fact that the lattice mismatch determined from the rocking curve is that corresponding to the structure of the epitaxial layer already adapted to the structure of the substrate. Since the lattice parameters of the epitaxial layer are larger than those of the substrate, the epitaxial laser is compressed to fit on the substrate.

3. Waveguide Fabrication and Characterization

To fabricate the planar waveguides, we first removed the epitaxial layer grown on one of the faces of the substrate. The epitaxial layer on the opposite face of the substrate was lapped down to a thickness of $\sim$23 μm and then polished, with alumina powders of grain size of 0.3 μm, to a final thickness of about 20 μm. The roughness of the polished epilayer was measured over an area of 5×5 mm^2, we obtained an rms value of 34 nm. The thickness of the epilayer was measured carefully with an optical imaging profiler (Sensofar, PLμ 300) by taking extended profiles from the substrate to the whole length of the epitaxial layer ($\sim$7 mm). We obtained a bend radius of 50 m which ensures a good flatness of epitaxial layer.

Monoclinic double tungstates are biaxial crystals and the binary axis of symmetry parallel to the **b** crystallographic direction is also parallel to one of the three crystallographic directions. The three principal optical directions are labeled N_g, N_m, and N_p. The N_g and N_m optical directions are located in the **a**−**c** crystallographic plane, while the N_p optical direction is perpendicular to that plane and is parallel to the **b** crystallographic direction. For KLuW as well as for KYbW, the N_g optical direction is located at 18.5° clockwise from the **c** crystallographic axis, and hence, the N_m optical direction (which is perpendicular to N_g) is located at an angle of 59.2° with respect to the **a** crystallographic axis.

Since we used substrates perpendicular to the **b** crystallographic direction, as explained before, our epitaxial layers grew with the N_p optical axis perpendicular to their surface, while the other two

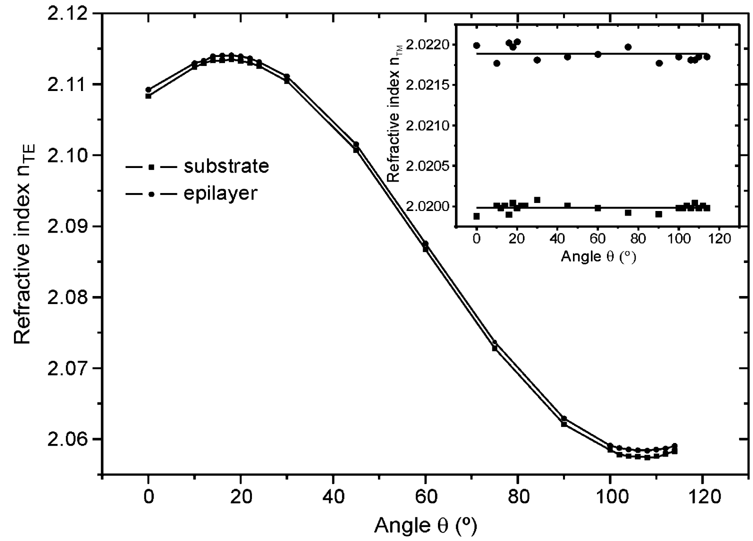

Fig. 3. Variation of the refractive indexes n_{TE} and n_{TM} (see inset) with the rotation angle of the sample measured in relation to the **c** crystallographic axis.

optical axes $\boldsymbol{N_g}$ and $\boldsymbol{N_m}$ are located in the same plane of the large surface of the sample. We measured the refractive indexes of the substrate and the epitaxial layer in these systems, at $\lambda = 632.8$ nm, with a METRICON 2010 prism film coupler. The laser beam in TE polarization allowed the measurement of the refractive indexes n_g and n_m associated with the optical directions $\boldsymbol{N_g}$ and $\boldsymbol{N_m}$, respectively, whereas the refractive index n_p associated with the optical direction $\boldsymbol{N_p}$ was determined by changing the polarization of the input beam to 90° or TM polarization. This was achieved by placing a half-wave plate in between the laser beam and the prism.

In order to locate precisely the position of the $\boldsymbol{N_g}$ and $\boldsymbol{N_m}$ directions in the epitaxial layer, as well as in the substrate, we also measured the refractive indexes as a function of θ, i.e., the angle formed by the **c** crystallographic axis and the TE polarization plane, e.g., when $\theta = 0$, the electric field oscillates parallel to the **c** crystallographic axis. This was done by rotating anticlockwise the sample beneath the prism around an axis perpendicular to its surface (this means parallel to the $\boldsymbol{N_p}$ optical direction) and parallel to the coupling head used to do pressure for the coupling process. The sample was rotated by steps of 15°, which were changed to 2° when the refractive index tended slowly to a maximum or a minimum, as shown in Fig. 3.

For TE measurements the maximum and minimum refractive index values were found to be at 18.5° ($\boldsymbol{N_g}$) and 108.5° ($\boldsymbol{N_m}$), respectively, from the **c** crystallographic axis for the substrate and the epitaxial layer. These results are in good agreement with the angles expected for the $\boldsymbol{N_g}$ and $\boldsymbol{N_m}$ directions to respect the **c** crystallographic axis. For TM polarization the refractive index does not seem to be affected by the rotation of the sample, as expected. The obtained values of the refractive indexes n_g, n_m, and n_p are summarized in Table 1.

As can be seen in Table 1 and Fig. 3, the refractive indexes of the film are greater than those of the substrate. The refractive index contrasts Δn_g, Δn_m, and Δn_p were 6×10^{-4}, 9×10^{-4}, and 1.9×10^{-3}, respectively, which are high enough to confine the light into the epitaxial layer, and hence, they would allow the demonstration of waveguiding properties of our 50 at.% Yb:KLuW/KLuW epitaxies.

We used the dark m-lines spectroscopy, which is also implemented in the system used to measure the refractive indexes, in order to characterize the waveguiding properties of the 50 at.% Yb:KLuW epitaxial layer. For the excitation of the different guided modes of the waveguide we also used light TE and TM polarized at 632.8 nm. The measurements were done by orienting the sample along the three principal optical directions found previously in Fig. 3. TE polarization enabled the study of guided modes supported by the epilayer with propagation of the light along the $\boldsymbol{N_g}$ and $\boldsymbol{N_m}$ directions. TM polarization enabled the study of the guided modes supported along the $\boldsymbol{N_p}$ direction. Table 1 also summarizes the effective refractive indexes determined using the acquisition

TABLE 1

Refractive indexes along the three principal optical directions and effective refractive indexes of guided modes supported by a 21-μm-thick 50% Yb:KLuW epilayer grown on a KLuW substrate

Direction	Polarization	Substrate refractive index at 632.8 nm	Film refractive index at 632.8 nm	Mode Order	Effective Refractive indices at 632.8 nm	Thickness [μm]
N_g	TE	2.1135(1)	2.1141(1)	0 1 2	2.1140 2.1138 2.1137	20.75 ± 1.03
N_m	TE	2.0575(1)	2.0584(2)	0 1 2 3	2.0584 2.0582 2.0580 2.0577	19.92 ± 0.71
N_p	TM	2.0200(1)	2.0219(1)	0 1 2 3 4 5	2.0219 2.0217 2.0215 2.0211 2.0207 2.0202	21.15 ± 0.16

software of the system together with the epitaxial layer thickness obtained by the dark mode measurements along the three optical axes.

At this wavelength, with a thickness of 20 μm, our waveguide can support up to three and four TE modes in N_g and N_m directions, respectively, whereas for TM polarization it can support up to six modes in N_p direction. The thicknesses for the epitaxial film obtained from the measurements along every principal optical direction are consistent, within the error, and coincides with the thickness of the epilayer measured by confocal microscopy.

To confirm our results and to establish the cutoff thickness to obtain a single mode waveguide, we performed a theoretical modeling of the effective refractive index of each guided mode as a function of the film thickness for the three polarizations analyzed in this work based on the theory developed in [21]. The results of this calculation are plotted in Fig. 4 for light TE polarized with E // N_g and N_m, as well as for light TM polarized with H // N_p.

The results plotted in Fig. 4 show that an epitaxial layer with a thickness of 20 μm (marked in each graph with a dotted line) acting as a planar waveguide can support up to three and four TE modes when electric field oscillates parallel to N_g and N_m directions, respectively, and up to six TM modes when magnetic field oscillates parallel to the N_p direction. Our modeling of the effective refractive indexes confirms the experimental results we obtained in Table 1 by the dark mode spectroscopy.

A rough estimation of the optical losses on these waveguides was performed along the three principal optical directions by coupling a He–Ne laser beam to the edge of the waveguide with microscope objectives of 20× and 40×, respectively. We recorded the scattered light along the propagation length in the waveguide with a CCD camera. The optical loses are due to propagated light scattered from the waveguide along its length. They can be attributed to several factors such as losses generated by the coupling of light into the waveguide through the microscope objectives, losses due to the high index contrast between the surface of the waveguide and air, and losses due to irregular scattering from defects at the interface between the epitaxial layer and the substrate. However, due to the low lattice mismatch characterized for these samples, of the order of 10^{-3}, we think that defects at the interface are not the main scattering source for these waveguides. The upper limit for losses in this waveguide was established to be at ~1.5 dB/cm. To reduce optical losses in these waveguides we propose to deposit a cladding with the same composition of the substrate on the top of the epitaxial layer, avoiding then the large refractive index contrast between the surface of the waveguide and air.

4. Conclusion

We demonstrated, for the first time to our knowledge, how heavily Yb^{3+}-doped KLuW layers (3.35×10^{21} Yb^{3+} ion/cm^3) could be used as passive slab waveguide at wavelengths that do not imply excitation of Yb^{3+}. The crystallographic characterization of these epilayers allowed us to determine a

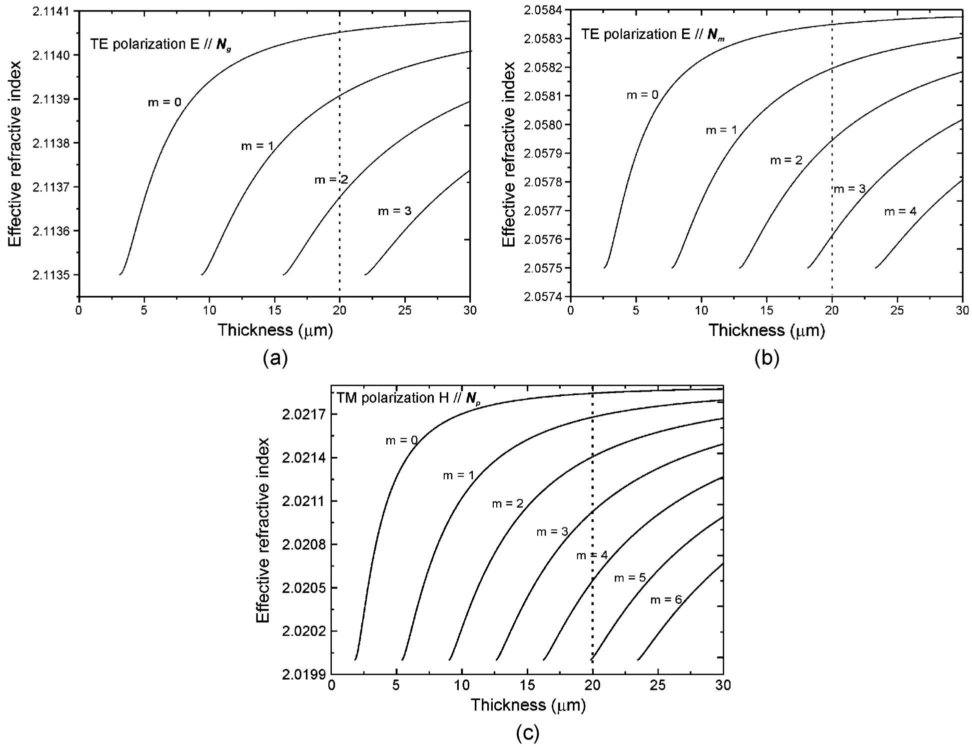

Fig. 4. Calculated effective refractive indexes of guided modes as a function of the thickness of the guiding layer thickness for the 50 at.% Yb:KLuW/KLuW system along the (a) $\boldsymbol{N_g}$, (b) $\boldsymbol{N_m}$, and (c) $\boldsymbol{N_p}$ principal optical directions.

very low lattice mismatch on the order of 10^{-3}, which indicated that these waveguides are almost lattice matched with the substrate. Also, the refractive index contrast we measured between the epitaxial layers and the substrate, which amounted to $6 \times 10^{-4} - 1.9 \times 10^{-3}$, depending on the direction of propagation, indicated that light confinement would be possible for these waveguides. We demonstrated experimentally that, effectively, up to three and four TE modes were supported by these waveguides in Ng and Nm directions, respectively, while up to six TM modes were supported in $\boldsymbol{N_p}$ direction for a 20-μm-thick Yb^{3+}: KLuW epilayer. The upper limit for optical losses in this waveguides was established to be at ~1.5 dB/cm, and we plan to reduce them by depositing a cladding on the top of the epitaxial layers that reduces the refractive index contrast between the epilayers and air.

Waveguiding is then another interesting application for these epilayers as it is the thin-disk laser [14]. We think that such waveguides may find application in on-chip integrated devices including other optical components.

In the future, we plan to explore the possibilities of obtaining guided laser emission from these heavily Yb^{3+}-doped KLuW epilayers by using a suitable excitation scheme.

References

[1] P. V. Klevtsov and L. P. Kozeeva, "Synthesis and X-ray and thermal studies of potassium rare-earth tungstates, $KLn(WO_4)_2$, Ln = rare-earth element," *Sov. Phys. - Dokl.*, vol. 14, pp. 185–187, Sep. 1969 [transl. from *Dokl. Akad. Nauk SSSR* 185, 571–574 (1969)].
[2] M. C. Pujol, X. Mateos, A. Aznar, X. Solans, S. Surinach, J. Massons, F. Díaz, and M. Aguiló, "Structural redetermination, thermal expansion and refractive indices of $KLu(WO_4)_2$," *J. Appl. Cryst.*, vol. 39, pp. 230–236, Mar. 2006.
[3] J. Zhang, J. Wang, K. Wang, W. Yu, H. Zhang, Z. Wang, X. Wang, and M. Ba, "Growth and structure of monoclinic $KLu(WO_4)_2$ crystals," *J. Cryst. Growth*, vol. 292, no. 2, pp. 373–376, Jul. 2006.
[4] V. Petrov, M. C. Pujol, X. Mateos, O. Silvestre, S. Rivier, M. Aguiló, R. M. Solé, J. Liu, U. Griebner, and F. Díaz, "Growth and properties of $KLu(WO_4)_2$, and novel ytterbium and thulium lasers based on this monoclinic crystalline host," *Laser Photon. Rev.*, vol. 1, pp. 179–212, May 2007.

[5] X. Mateos, R. Solé, J. Gavaldà, M. Aguiló, J. Massons, F. Díaz, V. Petrov, and U. Griebner, "Crystal growth, spectroscopic studies and laser operation of Yb^{3+}-doped potassium lutetium tungstate," *Opt. Mater.*, vol. 28, no. 5, pp. 519–523, Apr. 2006.
[6] U. Griebner, S. Rivier, V. Petrov, M. Zorn, G. Erbert, M. Weyers, X. Mateos, M. Aguiló, J. Massons, and F. Díaz, "Passively mode-locked $Yb:KLu(WO_4)_2$ oscillators," *Opt. Express*, vol. 13, pp. 465–3470, May 2005.
[7] X. Mateos, V. Petrov, J. Liu, M. C. Pujol, U. Griebner, M. Aguiló, F. Díaz, M. Galán, and G. Viera, "Efficient 2-μm continuous-wave laser oscillation of $Tm^{3+}:KLu(WO_4)_2$," *IEEE J. Quantum Electron.*, vol. 42, no. 10, pp. 1008–1015, Oct. 2006.
[8] A. A. Kaminskii, A. A. Pavlyuk, N. R. Agamalyan, L. I. Bobovich, A. V. Lukin, and V. V. Lyubchenko, "Stimulated emission by $KLu(WO_4)_2 - Er^{3+}$ crystals at room temperature," *Inorg. Mater.*, vol. 15, pp. 1182–1183, 1979.
[9] A. A. Kaminskii, A. A. Pavlyuk, N. R. Agamalyan, S. E. Sarkisov, L. I. Bobovich, A. V. Lukin, and V. V. Lyubchenko, "Stimulated radiation of Nd^{3+} and Ho^{3+} ions in monoclinic $KLu(WO_4)_2$ crystals at room temperature," *Inorg. Mater.*, vol. 15, p. 1649, 1979.
[10] A. A. Kaminskii, N. R. Agamalyan, A. A. Pavlyuk, L. I. Bobovich, and V. V. Lyubchenko, "Preparation and luminescence-generation properties of $KLu(WO_4)_2:Nd^{3+}$," *Inorg. Mater.*, vol. 19, pp. 885–894, 1983.
[11] A. A. Lagatsky, N. V. Kuleshov, and V. P. Mikhailov, "Diode-pumped CW lasing of Yb:KYW and Yb:KGW," *Opt. Commun.*, vol. 165, no. 1–3, pp. 71–75, Jul. 1999.
[12] U. Griebner, J. Liu, S. Rivier, A. Aznar, R. Grunwald, R. Solé, M. Aguiló, F. Díaz, and V. Petrov, "Laser operation of epitaxially grown $Yb:KLu(WO_4)_2 - KLu(WO_4)_2$ composites with monoclinic crystalline structure," *IEEE J. Quantum Electron.*, vol. 41, no. 3, pp. 408–414, Mar. 2005.
[13] A. Aznar, O. Silvestre, M. C. Pujol, R. Solé, M. Aguiló, and F. Díaz, "Liquid-phase epitaxy crystal growth of monoclinic $KLu_{1-x}Yb_x(WO_4)_2/KLu(WO_4)_2$ layers," *Cryst. Growth Des.*, vol. 6, no. 8, pp. 1781–1787, Jan. 2006.
[14] S. Rivier, X. Mateos, V. Petrov, U. Griebner, A. Aznar, O. Silvestre, R. Solé, M. Aguiló, F. Díaz, M. Zorn, and M. Weyers, "Mode-locked laser operation of epitaxially grown $Yb:KLu(WO_4)_2$ composites," *Opt. Lett.*, vol. 30, no. 18, pp. 2484–2486, Sep. 2005.
[15] Y. E. Romanyuk, C. N. Borca, M. Pollnau, S. Rivier, V. Petrov, and U. Griebner, "Yb-doped $KY(WO_4)_2$ planar waveguide laser," *Opt. Lett.*, vol. 31, pp. 53–55, Jan. 2006.
[16] F. M. Bain, A. A. Lagatsky, S. V. Kurilchick, V. E. Kisel, S. A. Guretsky, A. M. Luginets, N. A. Kalanda, I. M. Kolesova, N. V. Kuleshov, W. Sibbet, and C. T. A. Brown, "Continuous-wave and Q-switched operation of a compact, diode-pumped Yb^{3+}: $KY(WO_4)_2$ planar waveguide laser," *Opt. Express*, vol. 17, no. 3, pp. 1666–1670, Feb. 2009.
[17] J. J. Carvajal, B. Raghothamachar, O. Silvestre, H. Chen, M. C. Pujol, V. Petrov, M. Dudley, M. Aguiló, and F. Díaz, "Effect of structural stress on the laser quality of highly doped $Yb:KY(WO_4)_2/KY(WO_4)_2$ and $Yb:KLu(WO_4)_2/KLu(WO_4)_2$ epitaxial structures," *Cryst. Growth Des.*, vol. 9, no. 2, pp. 653–656, Jan. 2009.
[18] O. Silvestre, M. C. Pujol, R. Solé, W. Bolaños, J. J. Carvajal, J. Massons, M. Aguiló, and F. Díaz, "Ln^{3+}: $KLu(WO_4)_2/KLu(WO_4)_2$ epitaxial layers: Crystal growth and physical characterization," *Mater. Sci. Eng. B*, vol. 146, pp. 59–65, Jan. 2008.
[19] G. Keisser, *Optical Communications Essentials,* 1st ed. New York: McGraw-Hill, 2003.
[20] I. C. Bassignana and C. C. Tan, "Determination of epitaxic-layer composition and thickness by double-crystal X-ray diffraction," *J. Appl. Cryst.*, vol. 22, no. 3, pp. 269–276, Jan. 1989.
[21] P. K. Tien and R. Ulrich, "Theory of prism-film coupler and thin-film light guides," *J. Opt. Soc. Amer.*, vol. 60, no. 10, pp. 1325–1337, Oct. 1970.